Bioorganic & Medicinal Chemistry 17 (2009) 7769–7774

Contents lists available at ScienceDirect

Bioorganic & Medicinal Chemistry

journal homepage: www.elsevier.com/locate/bmc

# Structure-based virtual screening approach to the discovery of novel inhibitors of factor-inhibiting HIF-1: Identification of new chelating groups for the active-site ferrous ion

Sungmin Ko [a], Myung Kyu Lee [b], Dongkyu Shin [c,*], Hwangseo Park [a,*]

[a] Department of Bioscience and Biotechnology, Sejong University, 98 Kunja-Dong, Kwangjin-Ku, Seoul 143-747, Republic of Korea
[b] BioNanotechnology Research Center, Korea Research Institute of Bioscience and Biotechnology, 52 Eoeun-Dong, Yuseong-Gu, Daejeon 305-333, Republic of Korea
[c] CrystalGenomics Inc., Asan Institute for Life Sciences, 388-1 Pungnap-2dong, Songpa-gu, Seoul 138-736, Republic of Korea

ARTICLE INFO

*Article history:*
Received 20 August 2009
Revised 15 September 2009
Accepted 17 September 2009
Available online 20 September 2009

*Keywords:*
Virtual screening
Docking
FIH1
Inhibitor
Anemia

ABSTRACT

The inhibitors of factor-inhibiting HIF-1 (FIH1) have been shown to be useful as therapeutics for the treatment of anemia. We have been able to identify eight novel FIH1 inhibitors with $IC_{50}$ values ranging from 30 to 80 μM by means of the virtual screening with docking simulations under consideration of the effects of ligand solvation in the scoring function. The newly identified inhibitors are structurally diverse and have various chelating groups for the active-site ferrous ion including sulfonamide, carboxylate, *N*-benzo[1,2,5]oxadiazol-4-yl amide, and 2-[1,2,4]triazolo[3,4-*b*]][1,3,4]thiadiazol-3-yl-quinoline moieties. Each of these four structural classes has not been reported as FIH1 inhibitor, and therefore can be considered for further development by structure–activity relationship or *de novo* design methods. The interactions with the amino acid residues responsible for the stabilizations of the inhibitors in the active site are addressed in detail.



## 1. Introduction

Molecular oxygen is necessary for the survival of most organisms including human. A low level of intracellular $O_2$ concentration, which is called hypoxia, often leads to the cellular dysfunction and culminates in cell death.[1] The excess of molecular oxygen can also have a negative effect on cells due to the oxidative damage.[2,3] Therefore, intracellular oxygen concentrations should be maintained within a narrow range similar to the atmospheric $O_2$ partial pressure. In human cells, this delicate modulation is controlled by the activity of hypoxia-inducible factor 1 (HIF-1).[4–6] HIF-1 is thus a key regulator that mediates the intracellular oxygen concentrations by inducing the transcription of various target genes involved in angiogenesis, erythropoiesis, cell survival, and glucose metabolism.[7,8] In the case of cancer, the function of HIF-1 also plays a crucial role in tumor promotion because its target genes are responsible for tumor angiogenesis, invasion, and anaerobic energy metabolism. It is now well established that HIF-1 is present at a high level in various cancer cells to restore from the local hypoxic condition caused by a rapid cell proliferation and to supply enough nutrients to the core region of a cancer through the newly developed blood vessel. Therefore, the inhibition of HIF-1 activity has been considered as a therapeutic strategy for cancer.[9–12]

The function of HIF-1 is known to be regulated by factor-inhibiting HIF-1 (FIH1) that impairs the activity of HIF-1 by the hydroxylation of β-carbon of the conserved asparagine residue (Asn803) in the α-subunit of heterodimeric HIF-1 (HIF-1α).[13] FIH1 belongs to 2-oxoglutarate (2OG)-dependent dioxygenase superfamily and contains a none-heme iron at the catalytic center. During the hydroxylative inhibition of HIF-1α, it consumes molecular oxygen and 2OG with the release of $CO_2$ and succinate under the normoxic conditions. FIH1 can thus serve as a target for the development of therapeutic agents for anemia or ischemia because the enhancement of HIF-1 activity can promote the production of erythropoietin (EPO) that induces the formation of red blood cells and the development of new blood vessels. Indeed, FIH1 inhibitors have a high potential to be developed into anti-ischemic drugs targeting the normal cells suffering from hypoxia because FIH1 is more active on HIF-1α than the other hydroxylases under hypoxic conditions.[14]

X-ray crystallographic studies showed that two Nε atoms of His199 and His279 and an Oδ atom of Asp201 are coordinated to the central ferrous ion that plays a role of Lewis acid catalyst in a series of asparaginyl modification of HIF-1α.[15,16] The remaining three coordination sites should be occupied by water molecules in the resting form, and by molecular oxygen and 2OG during the catalytic reactions. Development of small-molecule FIH1 inhibitors

* Corresponding authors. Tel.: +82 2 3408 3766/3010 8626; fax: +82 2 3408 4334/3010 8601.
*E-mail addresses:* easar@cgxinc.com (D. Shin), hspark@sejong.ac.kr (H. Park).

0968-0896/$ - see front matter © 2009 Elsevier Ltd. All rights reserved.
doi:10.1016/j.bmc.2009.09.034

lags behind the biological and structural studies due mainly to the difficulty in designing a chelating group for the central ferrous ion. Only a few substrate-analog inhibitors of FIH1 have been reported so far. In this regard, earlier studies indicated that a cell-permeable 2OG analog such as dimethyl-oxalylglycine (DMOG) could block the asparaginyl hydrolase activity of FIH1.[13,17] *N*-oxalylglycine (NOG) is another known FIH1 inhibitor with millimolar activity although it can also inhibit the catalytic activities of most of enzymes in Fe(II)- and 2OG-dependent dioxygenase superfamily. A series of *N*-oxalyl amino acids have also been shown to be substrate-analog inhibitors of FIH1 with varying inhibitory activities.[18]

In the present study, we identify the novel classes of FIH1 inhibitors based on the computer-aided drug design protocol involving virtual screening with docking simulations and in vitro enzyme assay. Virtual screening has not always been successful due to the inaccuray in the scoring function, which leads to a weak correlation between the enrichment in virtual screening and binding mode prediction.[19] The characteristic feature that discriminates our virtual screening approach from the others lies in the implementation of an accurate solvation model in calculating the binding free energy between FIH1 and its putative inhibitors, which would have the effect of enhancing the hit rate in enzyme assay.[20] To further increase the accuracy in virtual screening, various energy parameters for the ferrous ion and its coordinated protein atoms will be developed with high-level quantum chemical calculations because they are unavailable in the current parameter database. To the best of our knowledge, we report the first example for the successful application of the structure-based virtual screening to identify the novel FIH1 inhibitors. It will be shown that the docking simulation with the improved binding free energy function can be a valuable tool for enriching the chemical library with molecules that are likely to have biological activities as well as for elucidating the observed activity of the identified inhibitors.

## 2. Experimental

As a receptor model for docking simulations, we chose the X-ray crystal structure of FIH1 in complex with the substrate 2OG (PDB entry: 1H2L)[15] from which 2OG and crystallographic water molecules had been removed. A special attention was paid to the assignment of the protonation states for the ionizable Asp, Glu, His, and Lys residues. The side chains of Asp and Glu residues were assumed to be neutral if one of their carboxylate oxygens pointed toward a hydrogen-bond accepting group including the backbone aminocarbonyl oxygen at a distance within 3.5 Å, a generally accepted distance limit for a hydrogen bond of moderate strength.[21] Similarly, the lysine side chains were assumed to be protonated unless the NZ atom was found in proximity of a hydrogen-bond donating group. The same procedure was also applied to determine the protonation states of ND and NE atoms in His residues. Atomic charges were then assigned to the all-atom model of FIH1 through the restrained electrostatic potential (RESP) methodology using the AMBER program.[22,23] Due to the lack of RESP charges for the central ferrous ion and its ligand groups, they were computed at RHF/6-31G* level of theory from the optimized geometry of the active-site ferrous ion cluster.

As a chemical library for virtual screening, we used the chemical database distributed by InterBioScreen (http://www.ibscreen.com), which comprises about 350,000 synthetic and natural compounds. Prior to the virtual screening with docking simulation, they were filtrated on the basis of Lipinski's 'Rule of Five' to adopt only the compounds with physicochemical properties of potential drug candidates and without reactive functional group(s).[24] To remove the structural redundancies in the chemical library, the structurally similar compounds with Tanimoto coefficient smaller than 0.1 were clustered into a single representative molecule. As a consequence, a docking library consisting of 120,000 compounds was constructed. These pre-filtrated compounds were subject to the CORINA program[25] to obtain their 3-D atomic coordinates, which was followed by the assignment of the atomic charges by means of the RESP method to be consistent with those of FIH1. We used the automated AUTODOCK program[26] in the virtual screening of FIH1 inhibitors because the outperformance of its scoring function over those of the others had been shown in several target proteins.[27] AMBER force field parameters were assigned for calculating the van der Waals interactions and the internal energy of a ligand as implemented in AUTODOCK. Iterative docking simulations were then carried out in the active site of FIH1 to score and rank the compounds in the docking library according to their calculated binding affinities.

In the actual docking simulations of the compounds in the docking library, we used the empirical AUTODOCK scoring function improved by the implementation of a new solvation model for a compound. The modified scoring function has the following form:

$$\begin{aligned}\Delta G^{\mathrm{aq}}_{\mathrm{bind}} = {} & W_{\mathrm{vdW}} \sum_i \sum_{j>i} \left( \frac{A_{ij}}{r_{ij}^{12}} - \frac{B_{ij}}{r_{ij}^{6}} \right) + W_{\mathrm{hbond}} \sum_i \sum_{j>i} E(t) \left( \frac{C_{ij}}{r_{ij}^{12}} - \frac{D_{ij}}{r_{ij}^{10}} \right) \\ & + W_{\mathrm{elec}} \sum_i \sum_{j>i} \frac{q_i q_j}{\varepsilon(r_{ij}) r_{ij}} + W_{\mathrm{tor}} N_{\mathrm{tor}} \\ & + W_{\mathrm{sol}} \sum_i^{\mathrm{atoms}} S_i \left( O_i^{\max} - \sum_{j>i}^{\mathrm{atoms}} V_j \mathrm{e}^{-\frac{r_{ij}^2}{2\sigma^2}} \right) \end{aligned} \quad (1)$$

Here, $W_{\mathrm{vdW}}$, $W_{\mathrm{hbond}}$, $W_{\mathrm{elec}}$, $W_{\mathrm{tor}}$, and $W_{\mathrm{sol}}$ are the weighting factors of van der Waals, hydrogen bond, electrostatic interactions, torsional term, and desolvation energy of inhibitors, respectively. $r_{ij}$ represents the interatomic distance, and $A_{ij}$, $B_{ij}$, $C_{ij}$, and $D_{ij}$ are related to the depths of the potential energy well and the equilibrium interatomic separations. The hydrogen bond term has an additional weighting factor, $E(t)$, representing the angle-dependent directionality to penalize the geometry unfavorable for the formation of a hydrogen bond. A cubic equation approach was applied to obtain the dielectric constant, $\varepsilon(r_{ij})$, required in computing the interatomic electrostatic interactions between FIH1 and a ligand molecule.[28] In the entropic term, $N_{\mathrm{tor}}$ is the number of $sp^3$ bonds in the ligand. In the desolvation term, $S_i$ and $V_i$ are the solvation parameter and the fragmental volume of atom $i$, respectively, while $Occ_i^{\max}$ stands for the maximum atomic occupancy. In the calculation of molecular solvation free energy term, we used the atomic parameters developed by Kang et al.[29] because those of the atoms other than carbon were unavailable in the current version of AUTODOCK. This modification of the solvation free energy term is expected to increase the accuracy in virtual screening because the underestimation of ligand solvation often leads to the overestimation of the binding affinity of a ligand with many polar atoms.[20] As a check for the accuracy of the present docking method, we carried out the docking simulation of NOG in the active site of FIH1 using the binding configuration in the original X-ray structure as the starting point. The results show that the root mean square deviation of the binding configuration from the X-ray structure falls into 1.0 Å, which supports the adequacy of the present docking simulations in virtual screening of the FIH1 inhibitors.

The inhibitory activities of the virtually screened compounds against FIH1 were measured with the monoclonal antibody-based screening assay developed by Lee et al.[30] This is very sensitive assay system using the monoclonal antibody, SHN-HIF1α, which binds to Asn803 hydroxylated HIF-1α in a specific fashion with at least 700-fold increase in binding affinity and 30-fold enhancement in sensitivity for screening FIH1 inhibitors when compared to the conventional methods. Each of the virtually screened compound was mixed with 10 mL of the enzyme solution (50 mM Tris

pH 7.5, 2 mM DTT, 0.22 mM FIH1, 220 mg/mL catalase, and 11 mM AFS) and incubated for 10 min at 37 °C. Ten milliliters of the substrate solution (50 mM Tris pH 7.5, 2 mM DTT, 2.2 mM bDES, 55 mM 2OG, and 1.1 mM ascorbate) were then added and further incubated for 20 min at 37 °C. The enzymatic reactions were stopped with the addition of 78 mL of 5 mM EDTA. The $IC_{50}$ values of the active compounds were measured by taking the average of duplicate experiments.

## 3. Results and discussion

To obtain the energy parameters of the active-site ferrous ion cluster that are required for modeling the binding of small molecules in the active site of FIH1, we followed the standard procedure to derive the potential parameters for metalloproteins.[31] The method involves geometry optimization of the simplified model for the ferrous ion in complex with the amino acid residues and the substrate at B3LYP/6-31G* level of theory. Figure 1 displays the structure of local energy minimum of the ferrous ion cluster whose input structures were taken from the X-ray structure of FIH1 in complex with 2OG.[15] The central ferrous ion reveals a distorted square pyramidal coordination with respect to the five ligand atoms, which is consistent with its coordination pattern in the original crystal structure. The sixth coordination position should be occupied by molecular oxygen to form a stable octahedral coordination. Interatomic distances associated with the central ferrous ion compare reasonably well with those in the crystal structure with a difference of 0.06 Å on average.

Table 1 lists the calculated RESP atomic charges of the central ferrous ion and its ligand atoms in the optimized structure of the complex. We note that the atomic charge of the ferrous ion decreases from +2.000 to +1.375 e upon the formation of the complex. On the other hand, those of the ligand atoms become less negative by 0.122 e for the nitrogen atoms of the two histidine residues, and by 0.123–0.214 e for the oxygen atoms of Asp201 and 2OG as compared to those in the absence of the ferrous ion. These changes reflect the redistribution of charges between the ferrous ion and its ligand atoms during the formation of the metal complex, exemplifying that the '$M^{n+}$' model for a metal ion is inadequate for describing the transition metal complexes in the active sites of metalloenzymes.[32] Therefore, we used the newly obtained atomic charges in the subsequent docking simulations of small-molecule ligands in the active site of FIH1 for virtual screening.

As a consequence of the virtual screening with docking simulations in the active site of FIH1, 200 top-scored compounds were selected as virtual hits. 189 compounds of them were available from the compound supplier and evaluated for in vitro inhibitory activity against recombinant human FIH1. In this experiment, the known FIH1 inhibitor quercetin was used as the reference. This in vitro enzyme inhibition assay for the virtual hits leads to the identification of 45 compounds that impairs the catalytic activity of FIH1 by more than 50% at the concentration of 500 μM. Most of the inactive compounds lack a proper chelating group for the active-site ferrous ion in the molecular structure. Among active compounds, eight compounds revealed a significant potency with the $IC_{50}$ values lower than 100 μM. The chemical structures and the inhibitory activities of the newly identified inhibitors are shown in Figure 2 and Table 2, respectively. We note that six (**1**–**6**) of the eight inhibitors include a thioxothiazolidinone moiety in the middle of their molecular structures. To the best of our knowledge, none of these compounds has been reported as FIH1 inhibitor so far. Although the inhibitory activities are moderate with the $IC_{50}$ values ranging from 30 to 80 μM, the newly found inhibitors are structurally diverse, and can be categorized into four structural classes according to the chelating group for the ferrous ion. Each of the structural classes can be considered as a new inhibitor scaffold for further development by structure–activity relationship (SAR) studies or *de novo* design.

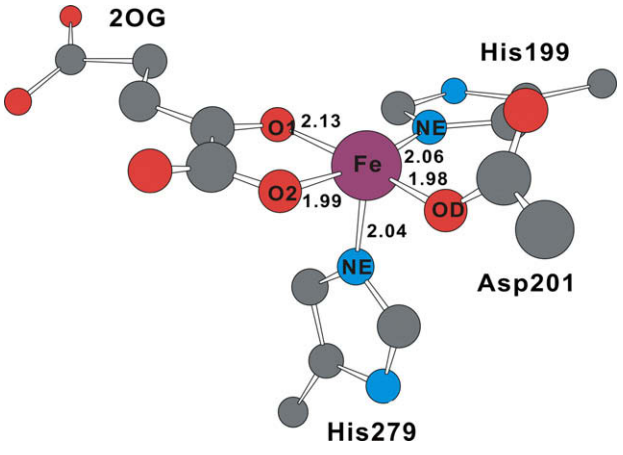


**Figure 1.** B3LYP/6-31G* optimized structure of the active-site ferrous ion cluster in complex with 2OG. The interatomic distances between the central ferrous ion and its ligand atoms are given in Å. All hydrogen atoms are omitted for visual clarity.

**Table 1**
Calculated RESP charges (in e) of the ferrous ion and its ligand atoms in the model system for FIH1-2OG complex

| Atoms | RESP charges |
|---|---|
| Fe | +1.375 (+2.000) |
| His199 NE | −0.350 (−0.472) |
| Asp201 OD | −0.547 (−0.761) |
| His279 NE | −0.350 (−0.472) |
| 2OG O1 | −0.476 (−0.599) |
| 2OG O2 | −0.595 (−0.778) |

Numbers in parentheses indicate the atomic charges before the formation of the metal complex.

To obtain structural insight into the inhibitory mechanisms for the identified inhibitors of FIH1, their binding modes in the active site were investigated using the AUTODOCK program. The inhibitors shown in Figure 2 were docked onto the active site of FIH1 from which the substrate 2OG had been removed. Although the distribution of the calculated binding modes is dependent on the number of rotatable bonds in molecular structures, most of the best-scored binding modes involve the chelation of the ferrous ion by a chemical group. These chelating groups include sulfonamide, carboxylate, *N*-benzo[1,2,5]oxadiazol-4-yl amide, and 2-[1,2,4]triazolo[3,4-*b*]][1,3,4]thiadiazol-3-yl-quinoline groups. Figure 3 compares the best-scored AUTODOCK conformations of the eight inhibitors shown in Figure 2. The results from the docking simulations are self-consistent in that the functional groups of similar chemical character are placed in similar ways with comparable interactions with the protein groups. As revealed by the superposition of their docked structures, for example, the chelating groups point toward the catalytic ferrous ion with the hydrophobic groups residing at the top of the active site. The proximity of the chelating groups to the ferrous ion in the best-scored conformations indicates their necessity in the inhibition of FIH1.

We now turn to the identification of the detailed interactions responsible for the stabilization of each inhibitor in the active site of FIH1. In the calculated FIH1-**1** complex shown in Figure 4, the nitrogen and one of the two oxygen atoms of the sulfonamide moiety are coordinated to the ferrous ion in the active site. This pattern for the coordination of sulfonamide group was also observed the inhibition of carbonic anhydrase that contains a zinc ion as a cofactor in the active site.[33] The remaining oxygen atom forms a bifurcated hydrogen bond with the side-chain amidic group of Asn205

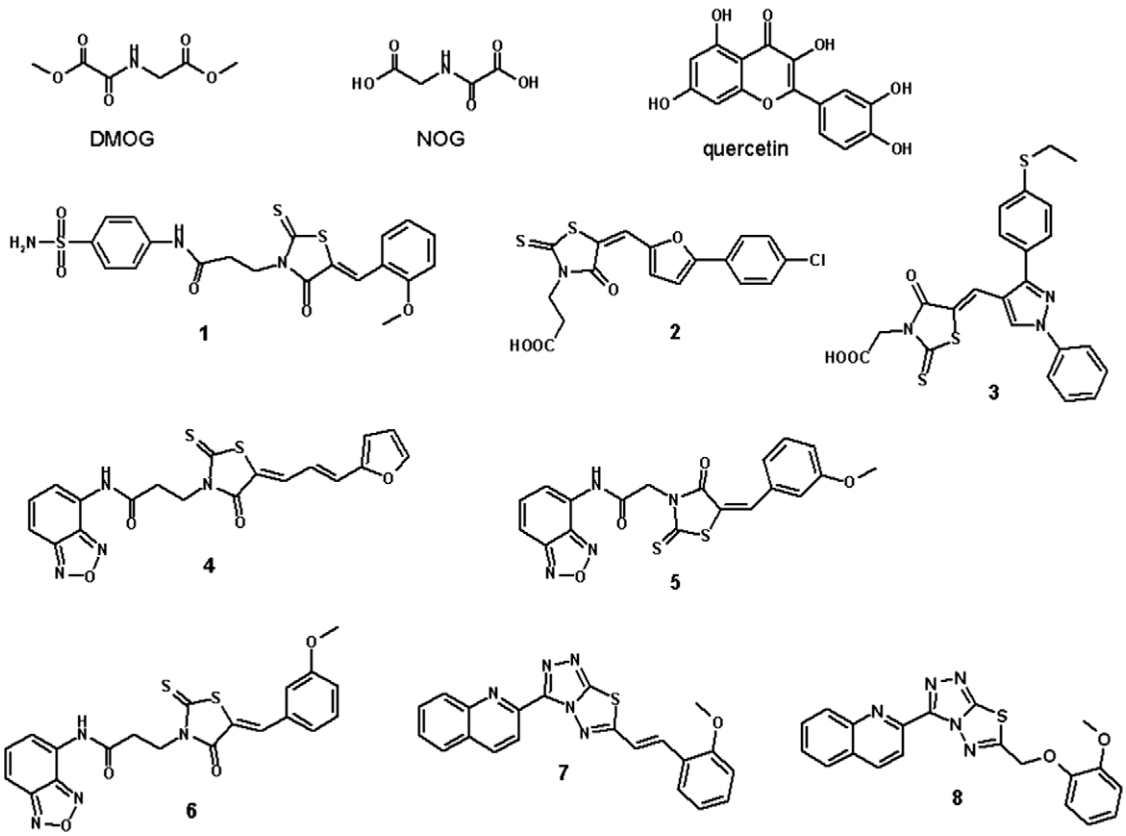


**Figure 2.** Chemical structures of the known and newly identified FIH1 inhibitors.

**Table 2**
$IC_{50}$ values (μM) of the reference and **1**–**8** against FIH1

| Compounds | $IC_{50}$ (μM) |
|---|---|
| Quercetin | 10.2 ± 0.7 |
| **1** | 32.1 ± 3.4 |
| **2** | 66.0 ± 4.2 |
| **3** | 36.2 ± 1.9 |
| **4** | 48.6 ± 5.3 |
| **5** | 45.3 ± 0.8 |
| **6** | 73.1 ± 7.6 |
| **7** | 47.5 ± 4.1 |
| **8** | 41.4 ± 2.9 |

and Asn294. This hydrogen bond seems to play a significant role in maintaining the coordination between the sulfonamide group and the ferrous ion as well as in stabilizing **1** in the active site of FIH1. Inhibitor **1** can be further stabilized in the active site by establishing the hydrophobic interactions of its aromatic rings with the nonpolar residues including Leu186, Leu188, and Trp296. On the basis of these structural features, it can be argued that **1** should be capable of impairing the enzymatic activity of FIH1 by binding in the active site through the simultaneous establishment of the multiple hydrogen bonds and hydrophobic interactions in addition to the chelation of the ferrous ion.

Figure 5 shows the lowest-energy binding mode of **2** in the active site of FIH1. In this case, the role of chelator for the central ferrous ion is played by the carboxylate group. Two oxygen atoms in the carbonyl and furan groups of the inhibitor receive the hydrogen bonds from the side-chain amidic nitrogen atoms of Asn294 and Gln147, respectively. A stable hydrogen bond is also established between the inhibitor sulfide moiety and the side-chain hydroxy group of Thr196. As in the FIH1-**1** complex, **2** forms van der Waals contacts with the side chains of Leu186, Leu188, and

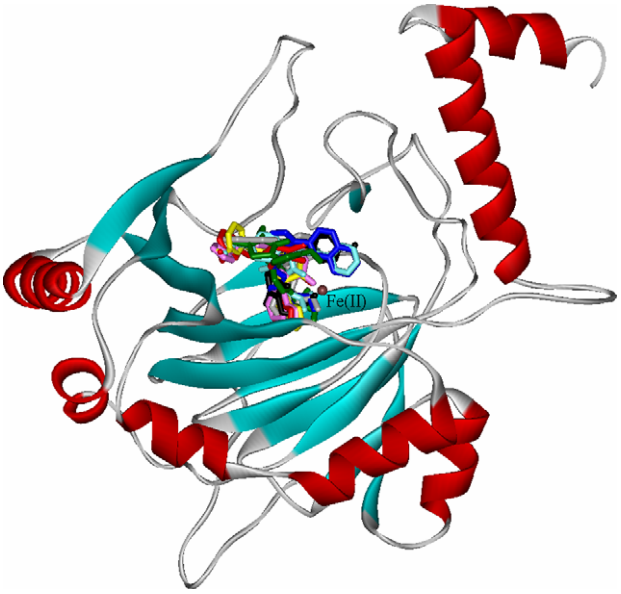


**Figure 3.** Comparative view of the binding modes of the newly found FIH1 inhibitors. Compounds **1**–**8** are indicated in green, black, cyan, pink, yellow, red, blue, and gray, respectively. The brown ball indicates the central ferrous ion.

Trp296, which should also be a significant binding force stabilizing **2** in the active site of FIH1.

The inhibitors **4**, **5**, and **6** are similar in structure and share *N*-benzo[1,2,5]oxadiazol-4-yl amide as a chelator for the central ferrous ion, the binding modes of which are compared in Figure 6. It is seen the aminocarbonyl oxygen and a benzoxadiazolyl nitrogen

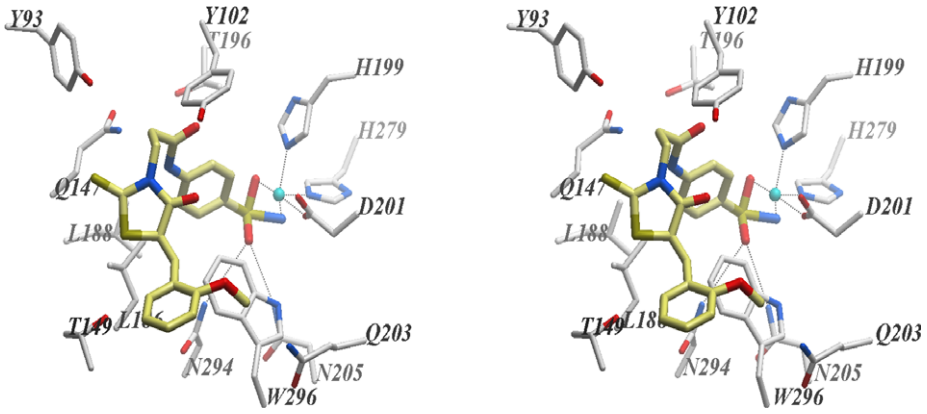


**Figure 4.** Binding mode of **1** in the active site of FIH1. Carbon atoms of the protein and the ligand are indicated in gray and yellow, respectively. Each dotted line indicates a hydrogen bond or a coordination to the central ferrous ion.

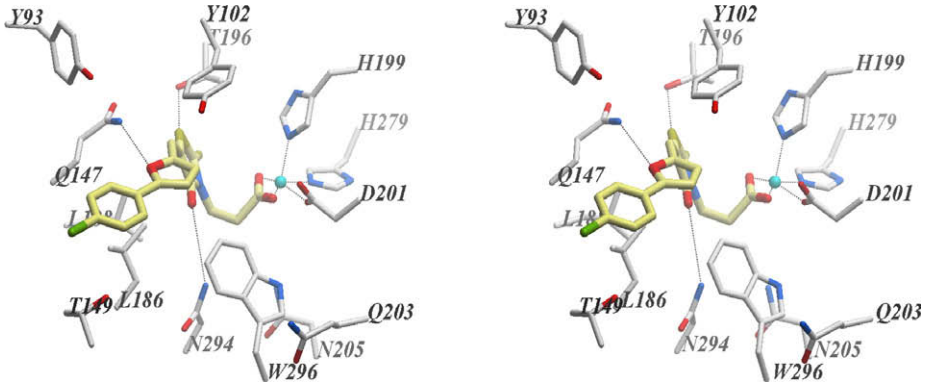


**Figure 5.** Binding mode of **2** in the active site of FIH1. Carbon atoms of the protein and the ligand are indicated in gray and yellow, respectively. Each dotted line indicates a hydrogen bond or a coordination to the central ferrous ion.

atoms are coordinated to the central ferrous ion in a simultaneous fashion. It is also a similar feature of binding modes that the common 2-thioxo-1,3-thiazolidin-4-one moiety plays a role of hydrogen-bond acceptor with respect to the side-chain amidic nitrogen of Gln147. The thiazolidine ring of the inhibitors is stacked between the side-chain aromatic rings of Trp296 and Tyr102. This kind of π-stacking has been considered as a significant binding force in the intermolecular interactions between biomolecules.[34] The side chain of Thr149 also plays a significant role in stabilizing the inhibitors in the active site by donating a hydrogen bond to the furan oxygen of **4** and the anisole oxygens of **5** and **6**.

The inhibitors **7** and **8** include the 2-[1,2,4]triazolo[3,4-*b*]][1,3,4]thiadiazol-3-yl-quinoline moiety that is likely to chelate the ferrous ion at the active site. However, this kind of coordination was not observed in the best-scored binding modes of **7** and **8** in which the anisole oxygen is instead coordinated to the ferrous ion. This is because the volume around the ferrous ion is insufficient in the present X-ray crystal structure to fully accommodate a large chelating group. To obtain the more probable binding modes of **7** and **8** with, therefore, further computational analyses should be performed under consideration of the structural flexibility of FIH1.

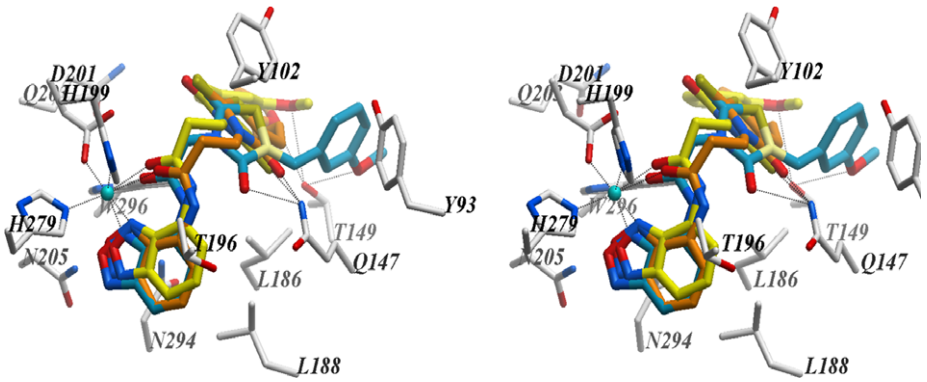


**Figure 6.** Comparative view of the binding modes of three compounds (**4**–**6**) in the active site of FIH1. Carbon atoms of **4**, **5**, and **6** are indicated in orange, yellow, and cyan, respectively. Each dotted line indicates a hydrogen bond or a coordination to the central ferrous ion.

## 4. Conclusions

We have identified eight novel inhibitors of FIH1 by applying a computer-aided drug design protocol involving the structure-based virtual screening with docking simulations under consideration of the effects of ligand solvation in the scoring function. These inhibitors are structurally diverse and can be categorized into four scaffolds according to the chelating group for the active-site ferrous ion. Because the inhibitory activities are found to be moderate with the $IC_{50}$ values ranging from 30 to 80 μM, each of the inhibitor scaffolds deserves a further development by structure–activity relationship studies or *de novo* design methods. Detailed binding mode analyses with docking simulations show that besides the chelation of the ferrous ion, the inhibitors can be stabilized in the active site by the simultaneous establishment of multiple hydrogen bonds with polar residues and van der Waals contacts with hydrophobic residues.

## References and notes


1. Wegner, R. H. *FASEB J.* **2002**, *16*, 1151.
2. Lefer, D. J.; Granger, D. N. *Am. J. Med.* **2000**, *109*, 315.
3. Hermes-Lima, M.; Zenteno-Sav, T. *Comp. Biochem. Phys. C* **2002**, *133*, 537.
4. Greijer, A. E.; van der Groep, P.; Kemming, D.; Shvarts, A.; Semenza, G. L.; Meijer, G. A.; van de Wiel, M. A.; Belien, J. A. M.; van Diest, P. J.; van der Wall, E. *J. Pathol.* **2005**, *206*, 291.
5. Semenza, G. L. *Sci. STKE* **2007**, *2007*, cm8.
6. Papandreou, I.; Cairns, R. A.; Fontana, L.; Lim, A. L.; Denko, N. C. *Cell Metab.* **2006**, *3*, 187.
7. Manalo, D. J.; Rowan, A.; Lavoie, T.; Natarajan, L.; Kelly, B. D.; Ye, S. Q.; Garcia, J. G. N.; Semenza, G. L. *Blood* **2005**, *105*, 659.
8. Pugh, C. W.; Ratcliffe, P. J. *Nat. Med.* **2003**, *9*, 677.
9. Semenza, G. L. *Nat. Rev. Cancer* **2003**, *3*, 721.
10. Harris, A. L. *Nat. Rev. Cancer* **2002**, *2*, 38.
11. Semenza, G. L. *Trends Mol. Med.* **2002**, *8*, S62.
12. Carroll, V. A.; Ashcroft, M. *Cancer Res.* **2006**, *66*, 6264.
13. Lando, D.; Peet, D. J.; Gorman, J. J.; Whelan, D. A.; Whitelaw, M. L.; Bruick, R. K. *Gene Dev.* **2002**, *16*, 1466.
14. Siddiq, A.; Ayoub, I. A.; Chavez, J. C.; Aminova, L.; Shah, S.; LaManna, J. C.; Patton, S. M.; Connor, J. R.; Cherny, R. A.; Volitakis, I.; Bush, A. I.; Langsetmo, I.; Seeley, T.; Gunzler, V.; Ratan, R. R. *J. Biol. Chem.* **2005**, *280*, 41732.
15. Elkins, J. M.; Hewitson, K. S.; McNeill, L. A.; Seibel, J. F.; Schlemminger, I.; Pugh, C. W.; Ratcliffe, P. J.; Schofield, C. J. *J. Biol. Chem.* **2003**, *278*, 1802.
16. Dann, C. E.; Bruick, R. K.; Deisenhofer, J. *Proc. Natl. Acad. Sci. U.S.A.* **2002**, *99*, 15351.
17. Milkiewicz, M.; Pugh, C. W.; Egginton, S. *J. Physiol.* **2004**, *560*, 21.
18. McDonough, M. A.; McNeill, L. A.; Tilliet, M.; Papamicael, C. A.; Chen, Q. Y.; Banerji, B.; Hewitson, K. S.; Schofield, C. *J. Am. Chem. Soc.* **2005**, *127*, 7680.
19. Warren, G. L.; Andrews, C. W.; Capelli, A. M.; Clarke, B.; LaLonde, J.; Lambert, M. H.; Lindvall, M.; Nevins, N.; Semus, S. F.; Senger, S.; Tedesco, G.; Wall, I. D.; Woolven, J. M.; Peishoff, C. E.; Head, M. S. *J. Med. Chem.* **2006**, *49*, 5912.
20. Shoichet, B. K.; Leach, A. R.; Kuntz, I. D. *Proteins* **1999**, *34*, 4.
21. Jeffrey, G. A. *An introduction to Hydrogen bonding*; Oxford University: Oxford, 1997.
22. Bayly, C. A.; Cieplak, P.; Cornell, W. D.; Kollman, P. A. *J. Phys. Chem.* **1993**, *97*, 10269.
23. Cornell, W. D.; Cieplak, P.; Bayly, C. I.; Gould, I. R.; Merz, K. M., Jr.; Ferguson, D. M.; Spellmeyer, D. C.; Fox, T.; Caldwell, J. W.; Kollman, P. A. *J. Am. Chem. Soc.* **1995**, *117*, 5179.
24. Lipinski, C. A.; Lombardo, F.; Dominy, B. W.; Feeney, P. J. *Adv. Drug Delivery Rev.* **1997**, *23*, 3.
25. Gasteiger, J.; Rudolph, C.; Sadowski, J. *Tetrahedron Comput. Methods* **1990**, *3*, 537.
26. Morris, G. M.; Goodsell, D. S.; Halliday, R. S.; Huey, R.; Hart, W. E.; Belew, R. K.; Olson, A. J. *J. Comput. Chem.* **1998**, *19*, 1639.
27. Park, H.; Lee, J.; Lee, S. *Proteins* **2006**, *65*, 549.
28. Park, H.; Jeon, J. H. *Phys. Rev. E* **2007**, *75*, 021916.
29. Kang, H.; Choi, H.; Park, H. *J. Chem. Inf. Model.* **2007**, *47*, 509.
30. Lee, S.-H.; Moon, J. H.; Cho, E. A.; Ryu, S.-E.; Lee, M. K. *J. Biomol. Screen.* **2008**, *13*, 494.
31. Fox, T.; Kollman, P. A. *J. Phys. Chem. B* **1998**, *102*, 8070.
32. Park, H.; Lee, S.; Suh, J. *J. Am. Chem. Soc.* **2005**, *127*, 13634.
33. Alterio, V.; Vitale, R. M.; Monti, S. M.; Pedone, C.; Scozzafava, A.; Cecchi, A.; Simone, G. D.; Supuran, C. T. *J. Am. Chem. Soc.* **2006**, *128*, 8329.
34. Waters, M. L. *Curr. Opin. Chem. Biol.* **2002**, *6*, 736.